Efficient Time-Domain and Frequency-Domain Finite-Element Solution of Maxwell's Equations Using Spectral Lanczos Decomposition Method

Mohammad R. Zunoubi, *Member, IEEE,* Kalyan C. Donepudi, Jian-Ming Jin, *Senior Member, IEEE,* and Weng Cho Chew, *Fellow, IEEE*

***Abstract*— An efficient three-dimensional solver for the solution of the electromagnetic fields in both time and frequency domains is described. The proposed method employs the edge-based finite-element method (FEM) to discretize Maxwell's equations. The resultant matrix equation after applying the mass-lumping procedure is solved by the spectral Lanczos decomposition method (SLDM), which is based on the Krylov subspace (Lanczos) approximation of the solution. This technique is, therefore, an implicit unconditionally stable finite-element time and frequency-domain scheme, which requires the implementation of the Lanczos process only at the largest time or frequency of interest. Consequently, a multiple time- and frequency-domain analysis of the electromagnetic fields is achieved in a negligible amount of extra computing time. The efficiency and effectiveness of this new technique are illustrated by using numerical examples of three-dimensional cavity resonators.**

***Index Terms*— Finite-element method, Maxwell's equations, spectral Lanczos decomposition method.**

I. Introduction

THE finite-difference time-domain (FDTD) technique, first introduced by Yee [1], has been the most popular method for the simulation of transient electromagnetic-wave phenomena for the past few decades. Despite its programming simplicity, ease in bookkeeping, and the simplicity of its numerical integration algorithm, it has suffered from the staircasing approximation in its original form when modeling curved surfaces [2]. Recent efforts have focused on the development of FDTD-based algorithms for irregular grids that conform to the surfaces of all boundaries in the problem domain [3]–[14]. Additionally, the FDTD is an explicit scheme, which is only conditionally stable.

To circumvent the aforementioned difficulties, the time-domain finite-element method (TD-FEM) has been proposed over the past ten years. A point-matched TD-FEM using conformal meshes was first introduced by Cangellaris *et al.* [15], [16] and was then extended to treat lossy media by Lin and Mei [17]. The major drawback of this technique is that all three components for each of the fields are placed at the same node, thus requiring special treatment for updating the nodes residing on surfaces where the electromagnetic properties of the media change abruptly [18]. Other finite-element time-domain (FETD) techniques which followed utilized an approximate diagonalization of the mass matrix to reduce the computational burden required for matrix solutions [19], [20]. A time-domain integration of Maxwell's equations on finite elements was reported by Lynch and Paulsen [21], which employed a generalized wave equation in weak form and used an integral lumping to render the mass matrix diagonal. This is an explicit scheme requiring no matrix solution, and a frequency-domain nodal-based finite-element code can be adapted to this time-domain technique [18]. It has, however, an uncertain accuracy and, furthermore, special treatment is necessary for material discontinuities since it is a nodal-based technique, and it has the potential of producing significant errors when perfectly conducting corners and edges are present [18].

To annihilate the problems described above and to offer more robust techniques, the use of edge elements was prescribed for finite-element treatment of Maxwell's equations [22] and was extended to the time-domain analysis. Mur [23] reported an edge-based FETD method where a second-order differential equation in time is solved by using a central difference formula. However, a contamination of the field signature with spurious linear-in-time signals was observed when the method was employed to analyze a resonating cavity [24]. Consequently, Mahadevan *et al.* [24] introduced an edge/face-based technique, which complemented the edge basis functions with face basis functions. Several other variants have been proposed and implemented, including the work by Elson *et al.* [25], Lee [26], [27], Wong *et al.* [28], and Feliziani and Maradei [29]. As a common technique, the time derivatives were approximated by a difference scheme, resulting in an explicit time-domain phenomenon. Therefore, the methods described above are only conditionally stable with time steps, which are typically equal to or smaller than those imposed by the FDTD technique. Implicit time-domain schemes, on the other hand, involve the solution of a matrix equation for every time step, while allowing for the possibility of implementing procedures that are unconditionally stable [18]. Such methods have been developed by Gedney and Navsariwala [30] for the solution of the vector-wave equation

Manuscript received June 17, 1997; revised January 26, 1998. This work was supported by the AFOSR under a grant from the MURI Program under Contract F49620-96-1-0025, the Office of Naval Research under Grant N00014-95-1-0848, and by the National Science Foundation under Grant ECS 94-57735.

The authors are with the Center for Computational Electromagnetics, Department of Electrical and Computer Engineering, University of Illinois at Urbana-Champaign, Urbana, IL 61801-2991 USA.

Publisher Item Identifier S 0018-9480(98)05505-7.

to analyze simple cavity resonators. Although the number of time steps is small, no comparison of the central processing unit (CPU) time is illustrated.

For an implicit method to be computationally as efficient as an explicit method, either the number of time iterations necessary for convergence must be very small [30] (since for each time iteration a solution of a linear systems of equations is required) or the system should be treated in a very efficient manner.

Recently, Zunoubi *et al.* [31], [32] have employed a spectral Lanczos decomposition method (SLDM) [33] for solving axisymmetric and three-dimensional low-frequency electromagnetic diffusion by the FEM. It has been demonstrated [31], [32] that the SLDM is very fast and is capable of obtaining solutions at many frequencies in a negligible amount of extra computing time.

In this paper, an edge-based FEM is employed to discretize Maxwell's equations in both time and frequency domains. The techniques are referred to as the FETD and the finite-element frequency-domain (FEFD), respectively. A matrix equation is obtained and the lumping procedure is applied to the mass matrix. The SLDM is then employed to solve for the electromagnetic fields for multiple times and frequencies implicitly. The efficiency and validity of this technique are tested by studying the resonant frequencies of various microwave cavities. Slight inaccuracy introduced in the time-domain signals by the mass-lumping approximation is also demonstrated.

II. Finite-Element Formulation

When electromagnetic problems are analyzed by the FEM, Maxwell's equations can be discretized by edge-based elements. In this section, such a discretization method is discussed. It is well known that Maxwell's equations in space–time $\Re^4$ are

$$\begin{aligned}\nabla \times \mathbf{E} &= -\mu \frac{\partial \mathbf{H}}{\partial t} \\ \nabla \times \mathbf{H} &= \mathbf{J} + \epsilon \frac{\partial \mathbf{E}}{\partial t} + \sigma \mathbf{E}.\end{aligned} \tag{1}$$

In a lossless medium, if (1) is solved for the electric-field intensity, we can write

$$\nabla \times \left(\frac{1}{\mu} \nabla \times \mathbf{E}\right) + \epsilon \frac{\partial^2 \mathbf{E}}{\partial t^2} = -\frac{\partial \mathbf{J}}{\partial t} \tag{2}$$

with the boundary conditions

$$\begin{aligned}\hat{n} \times \mathbf{E} &= 0 \text{ on electric walls} \\ \hat{n} \times \nabla \times \mathbf{E} &= 0 \text{ on magnetic walls.}\end{aligned} \tag{3}$$

The solution of (2) and (3) is obtained by seeking the stationary point of the functional given by [34]

$$F(\mathbf{E}) = \frac{1}{2} \iiint_V \left[\frac{1}{\mu}(\nabla \times \mathbf{E}) \cdot (\nabla \times \mathbf{E}) + \epsilon \mathbf{E} \cdot \frac{\partial^2}{\partial t^2} \mathbf{E}\right] dV + \iiint_V \frac{\partial \mathbf{J}}{\partial t} \cdot \mathbf{E}\, dV \tag{4}$$

where V denotes the volume of interest. This functional can be discretized by first subdividing the volume V into small elements and expanding the electric field as

$$\mathbf{E}(x, y, z) = \sum_{i=1}^{N} \mathbf{N}_i(x, y, z) E_i \tag{5}$$

where $\mathbf{N}_i$ denotes the expansion function associated with edge i, E_i denotes the associated tangential electric field, and N denotes the total number of edges in V. Substituting (5) into (4) and applying the Rayleigh–Ritz procedure, we obtain the matrix equation

$$\left([C] + \frac{d^2}{dt^2}[T]\right)\{E\} = \frac{d}{dt}\{b\} \tag{6}$$

where $\{E\} = [E_1, E_2, \cdots, E_N]^T$ and

$$\begin{aligned}C_{i,j} &= \iiint_V \frac{1}{\mu}(\nabla \times \mathbf{N}_i) \cdot (\nabla \times \mathbf{N}_j)\, dV \\ T_{i,j} &= \iiint_V \epsilon(\mathbf{N}_i \cdot \mathbf{N}_j)\, dV \\ b_i &= -\iiint_V (\mathbf{N}_i \cdot \mathbf{J})\, dV.\end{aligned} \tag{7}$$

The $[C]$ and $[T]$ in (6) are the *stiffness* and *mass* matrices, respectively. This matrix equation can be solved after mass lumping by the SLDM, which is discussed in detail in Section III.

III. SLDM

In order to solve (6) for the electric field by the SLDM [33], this equation must first be cast into a form

$$\left(A + \frac{d^2}{dt^2} I\right)x = \frac{d}{dt} u \tag{8}$$

with I being the identity matrix. Therefore, the matrix T of (6) is first converted into a diagonal matrix by the row–sum lumping procedure to yield

$$\left(C + \frac{d^2}{dt^2} D\right)E = \frac{d}{dt} b. \tag{9}$$

In the row–sum lumping procedure, the diagonal entries of matrix D are determined as the sum of all the elements in the corresponding rows of matrix T. For the sake of convenience, we omit the brackets for the notation of matrices and vectors in this section. Equation (9) can be further written as

$$\left(D^{-1/2} C D^{-1/2} + \frac{d^2}{dt^2} I\right)E' = D^{-1/2} \frac{d}{dt} b \tag{10}$$

or

$$\left(A' + \frac{d^2}{dt^2} I\right)E' = \frac{d}{dt} b' \tag{11}$$

with $E' = D^{1/2}E$ and $b' = D^{-1/2}b$, assuming that no zero or negative elements are present on the diagonal of matrix D. If we define

$$b'(\mathbf{r}, t) = b'(\mathbf{r})[u(t) - u(t - T)] \tag{12}$$

where u denotes a unit step function, following the Laplace transform of (11), we can write

$$[s^2 I + A']E'(s) - \dot{E}'(0) = -b'(\mathbf{r}) e^{-Ts}. \tag{13}$$

In the above, $E'(0) = 0$ and $\dot{E}'(0)$ is determined to be $b'(\mathbf{r})$ so that

$$E'(s) = b'(\mathbf{r})\left[\frac{1 - e^{-Ts}}{s^2 I + A'}\right]. \tag{14}$$

Applying the inverse Laplace transform yields

$$E'(t) = \frac{b'(\mathbf{r})}{\sqrt{A'}}\left[\sin\sqrt{A'}t - \sin\sqrt{A'}(t-T)\right]. \tag{15}$$

It is evident that the electric-field intensity $\mathbf{E}$ can be analytically determined in both frequency and time domains from (14) and (15), respectively. Note that the time dependence in (12) is not the only choice; other time functions can be chosen as well. For example, if a modulated exponential decay function such as

$$b'(\mathbf{r}, t) = b'(\mathbf{r})[e^{-at}\sin(bt)u(t)] \tag{16}$$

is chosen, then we can write

$$E'(s) = b'(\mathbf{r})\left\{\frac{bs}{(A' + s^2 I)[b^2 + (a+s)^2]}\right\} \tag{17}$$

and

$$\begin{aligned} E'(t) = {} & \frac{b'(\mathbf{r})e^{-at}}{(a^2+b^2)^2 + (2a^2 - 2b^2 + A')A'} \\ & \cdot\Big[-(a^3 + ab^2 + aA')\sin(bt) \\ & -(a^2 b + b^3 - bA')\cos(bt) + e^{at}(a^2 b + b^3 - bA') \\ & \cdot\cos(\sqrt{A'}t) + 2ab\sqrt{A'}\sin(\sqrt{A'}t)\Big]. \end{aligned} \tag{18}$$

The unknown vector E' in the above equations is approximated in the SLDM by replacing the matrix A' with its $M(<N)$ eigenvalues and corresponding eigenvectors. Additionally, the eigenpairs are not calculated directly from the symmetric matrix A', but from a symmetric tridiagonal matrix, which is generated from A' via an orthogonal transformation or, more specifically, the Lanczos process. The tridiagonal matrix H is the Ritz approximation of A' and is related to A' as

$$Q^T A' Q = H \tag{19}$$

where $Q = [q_1, q_2, \cdots, q_M]$ is an orthogonal matrix. The bases $q_1, q_2, \cdots, q_M$ are generated by the Gram–Schmidt orthogonalization process of vectors b', $A'b'$, $\cdots$, $A'^{M-1}b'$ in the Krylov subspace

$$\kappa(A', q_1, M) = \text{span}\{q_1, A'q_1, \cdots, A'^{M-1}q_1\}. \tag{20}$$

Next, we define the elements of the Ritz matrix H as

$$\begin{aligned} H_{i,i} &= \alpha_i, \qquad i = 1, 2, \cdots, M, \\ H_{i,i-1} &= H_{i-1,i} = \beta_i, \qquad i = 1, 2, \cdots, M-1 \end{aligned} \tag{21}$$

so that (19) can be expressed as

$$A'q_i = \beta_{i-1}q_{i-1} + \alpha_i q_i + \beta_i q_{i+1}, \qquad i = 1, 2, \cdots, M \tag{22}$$

where $\beta_0 q_0 = 0$. The orthonormality of q_i implies that

$$\alpha_i = q_i^T A' q_i. \tag{23}$$

If we define

$$r_i = (A' - \alpha_i I)q_i - \beta_{i-1}q_{i-1} \neq 0 \tag{24}$$

we can then express q_{i+1} as

$$q_{i+1} = \frac{r_i}{\beta_i} \tag{25}$$

where $\beta_i = \|r_i\|_2$. Equations (21)–(25) define the Lanczos process which is used to construct the tridiagonal matrix H and the orthogonal matrix Q. If we further define Λ and V to be the eigenvalues and their corresponding eigenvectors of matrix H, respectively, then we can write

$$H = V\Lambda V^T, \qquad \Lambda = \text{diag}[\lambda_1, \lambda_2, \cdots, \lambda_M] \tag{26}$$

and choose a vector q_1 as

$$q_1 = Qe_1 = \frac{b'}{\|b'\|} \tag{27}$$

where $e_1 = (1, 0, 0, \cdots, 0)^T$ is the first unit M vector. The unknowns $E'(s)$ and $E'(t)$ in (14) and (15) can then be approximated by

$$E'(s) = \|b'\|QV\left[\frac{1 - e^{-Ts}}{s^2 I + \Lambda}\right]V^T e_1 \tag{28}$$

and

$$E'(t) = \|b'\|QV\left[\frac{\sin\sqrt{\Lambda}t - \sin\sqrt{\Lambda}(t-T)}{\sqrt{\Lambda}}\right]V^T e_1 \tag{29}$$

respectively. These are valid approximations of the unknown vectors $E'(s)$ and $E'(t)$ since the spectrum of H is contained in the spectral segment of matrix A'. The corresponding expressions for (17) and (18) can be similarly obtained.

The main arithmetic work in the SLDM is to obtain matrices Q and H. However, the dimension of the Krylov subspace M necessary to reach convergence is typically much smaller than the dimension of matrix A' [33]. For efficient computations of the eigenvalues and eigenvectors of matrix A', the PWK [35] and inverse-iteration algorithms are implemented. With the above algorithms used to compute the eigenpairs of matrix A, only $O(M^2)$ operations are required. Additionally, it is not necessary to recompute Q and H matrices for multiple frequencies or time steps. Only the matrix functionals $f(H)$ of (28) and (29) need to be computed for various frequencies and time steps. This proves to be the most attractive feature of the SLDM. This fact is further verified in Section IV.

IV. Results

To verify the formulation presented in this paper, the resonant frequencies of various microwave cavities are studied. First, a rectangular air-filled cavity, for which the resonant frequencies are known analytically, is studied. Second, an inhomogeneous cavity is simulated and the results are compared with the corresponding results reported in [36]. The electric-field intensity is determined in both frequency and time domains. Very accurate results are obtained in minimal computational time. All the computations are performed on a DEC Alpha Workstation computer with an average throughput of 44 MFlops and the tolerance (the relative difference between two consecutive iterations) used to terminate the SLDM iterations is 10^{-8}.

A. Rectangular Cavity

A rectangular cavity with unequal side lengths is first considered. The problem geometry is illustrated in Fig. 1. The

TABLE I
RESONANT FREQUENCIES OF A 5 m × 4 m × 3 m CAVITY RESONATOR USING FREQUENCY-DOMAIN ANALYSIS

Mode	011	101	110	111	012	102	021	112	120	121	022	013
Exact (MHz)	48.0	58.3	62.5	69.3	70.8	78.1	80.7	86.6	90.1	95.0	96.0	97.5
FEFD (MHz)	47.9	58.1	62.3	69.1	70.4	77.6	80.3	86.2	89.4	94.2	95.0	96.6
% Error	0.21	0.34	0.32	0.29	0.56	0.64	0.49	0.58	0.84	0.78	1.04	0.92

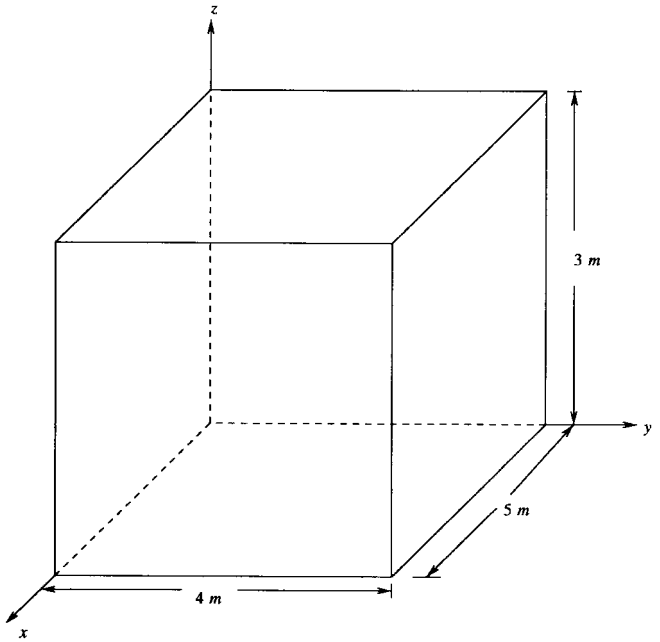

Fig. 1. The problem geometry for the electric field computation of an air-filled resonant cavity.

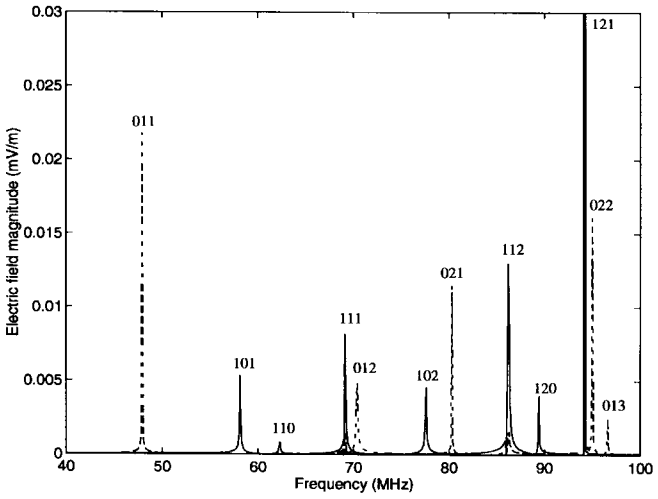

Fig. 2. Typical frequency spectrum of a 5 m × 4 m × 3 m resonant cavity.

TABLE II
RESONANT FREQUENCIES OF A 5 m × 4 m ××3 m CAVITY RESONATOR USING TIME-DOMAIN ANALYSIS

Mode	011	102	112	120	121	013	121
Exact (MHz)	48.0	58.3	69.3	78.1	86.6	90.1	95.0
FETD (MHz)	48.7	57.1	69.0	77.2	85.3	89.3	93.4
% Error	1.46	2.06	0.43	1.15	1.50	0.89	1.68

cavity dimensions are 5 m × 4 m × 3 m, which are subdivided into 20, 16, and 12 segments, respectively. The total number of unknowns is, therefore, 10 064. The cavity is illuminated by a short pulse of duration $T = 1.443375$ ns positioned near a corner in order to excite as many resonant modes as possible.

First, the magnitude of the electric field is computed from (28) at the largest frequency of interest—100 MHz—while the same Q and H matrices are used to calculate the field in a frequency range of 40–100 MHz with a frequency increment of 0.1 MHz. The frequency spectrum of the field is given in Fig. 2. The total CPU time required to obtain results of Fig. 2 is only 65.6 s, of which 56.6 s are spent on the first frequency point and only 9.0 s are spent on the remaining 599 frequency points. Similar results were obtained using the Whitney-element time-domain (WETD) method [27] with a CPU time of approximately 13 418 s on an HP-735 Workstation. A comparison of the computed resonant frequencies with the analytical values is given in Table I. As can be seen from this table, the numerical results are very accurate.

Next, the electric-field intensity is calculated by the SLDM from (29) at the largest time of interest, 0.24 μs and a multiple-time analysis is performed for $t = 0.0$ to 0.24 μs with a time step of $\Delta t = 0.481\,125$ ns using the same Q and H matrices obtained at $t = 0.24$ μs. The field is sampled at a few locations inside the cavity and the Fourier transform of the time-domain response is performed, which clearly indicates the resonance peaks, from which the resonant frequencies can be determined. The numerical and analytical resonant frequencies are listed in Table II. Again, excellent agreement is observed. The total CPU time is 131.5 s, of which 122 s are spent on the first time point, and 9.5 s are spent on the remaining 499 time points. The longer CPU time is due to the calculation of the sine functions and square root in (29).

To examine the accuracy of the waveform calculation using (29), the electric field computed at the center of the cavity for the first 300 time steps is compared with the corresponding results obtained from the conventional finite-difference time-domain (FDTD) method. Note that the same time step as for the FEM analysis is chosen for the FDTD computations. To also enforce the constrain of 20 cells per wavelength imposed in the FDTD technique, we pass the short pulse through a finite impulse response (FIR) low-pass filter [37] with a cutoff frequency of 60.0 MHz. This will eliminate the possibility of contaminating the time-domain signal by the high-frequency components of the field.

Results are depicted in Fig. 3. As can be seen from this figure, the general agreement is very good and there is only a slight disagreement between the two solutions. To identify the

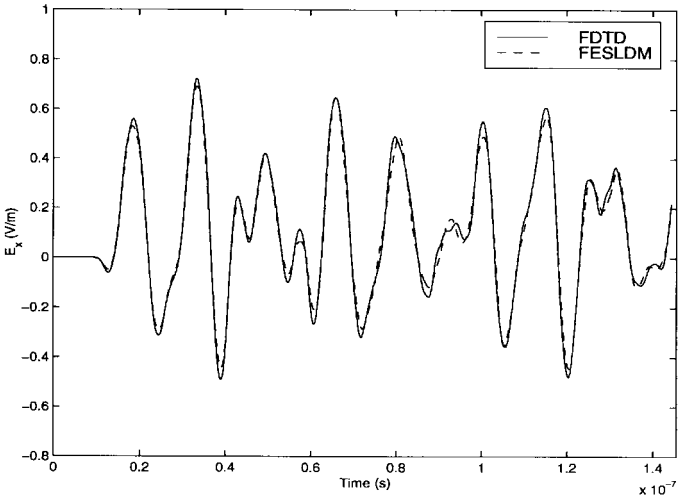

Fig. 3. A comparison of the FESLDM and FDTD response of the air-filled cavity excited by a filtered short pulse.

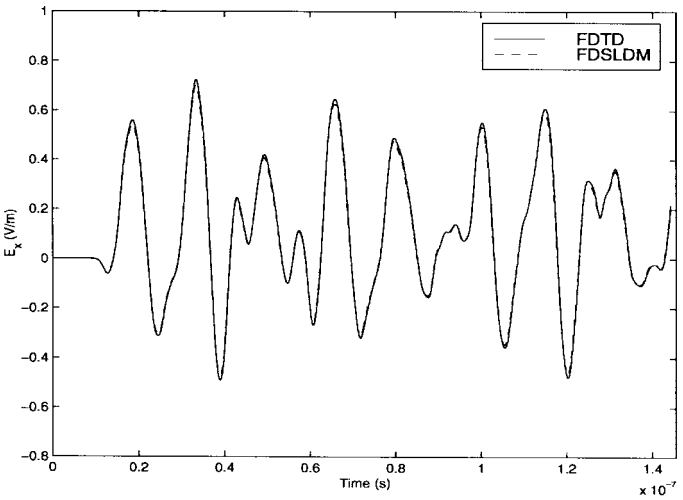

Fig. 4. A comparison of the FDSLDM and FDTD response of the air-filled cavity excited by a filtered short pulse.

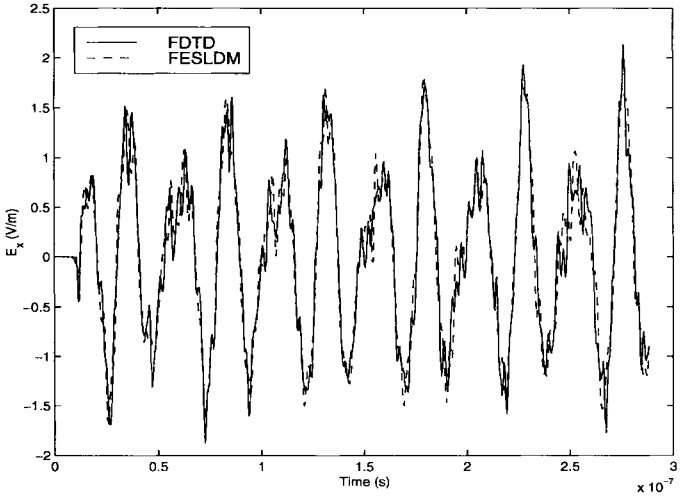

Fig. 5. A comparison of the FESLDM and FDTD response of the air-filled cavity excited by a tapered sine function.

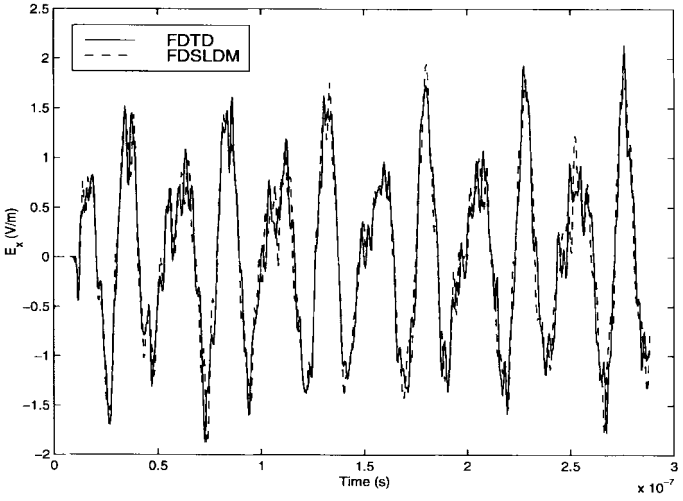

Fig. 6. A comparison of the FDSLDM and FDTD response of the air-filled cavity excited by a tapered sine function.

possible source of this small error, we note that (29) contains $\sin\sqrt{\Lambda}t$ and $\cos\sqrt{\Lambda}t$. The accuracy of the calculation of these two terms depends not only on the relative accuracy of Λ, but also on the absolute value of Λ. A very small relative error in Λ can cause a significant error in the calculation of $\sin\sqrt{\Lambda}t$ and $\cos\sqrt{\Lambda}t$ when Λ and t are large. Therefore, in order to calculate $E'(t)$ using (29) accurately, one must calculate Λ very accurately. However, the accuracy of Λ is limited by the numerical discretization, especially by the mass-lumping procedure for large Λ's.

To verify this point, we applied the finite-difference scheme to (2), which results in an equation identical to (8) without a need for mass lumping. The resulting equation is then solved by the SLDM, as described in Section III. The electric field computed at the cavity center is compared with the FDTD results and the comparison is given in Fig. 4. As can be seen from this figure, an excellent agreement is achieved because, by avoiding the mass-lumping procedure, the high eigenvalues (Λ) are computed more accurately.

As another example, a tapered sine function

$$b'(\mathbf{r}, t) = b'(\mathbf{r})[(1 - e^{-at})\sin(bt)u(t)] \tag{30}$$

is used as the excitation, where $a = 0.261\,187 \times 10^9$ and $b = a/5$. Note that here, the 20 cells per wavelength constraint has been already enforced. The x-component of the electric field is computed by both FESLDM and FDSLDM and the results are compared with the corresponding FDTD results. Comparisons are given in Figs. 5 and 6, respectively. A good agreement is obtained for the FESLDM results. When a low-pass FIR filter with a cutoff frequency of 120.0 MHz is used to remove the high-frequency components that are not modeled accurately with the numerical discretization, results are excellent, as can be seen in Figs. 7 and 8.

To justify the multiple time and frequency analysis, the SLDM is employed to compute the field at each single frequency and time in the frequency range of 40–100 MHz and time range of 0–0.24 μs, and the number of the SLDM it-

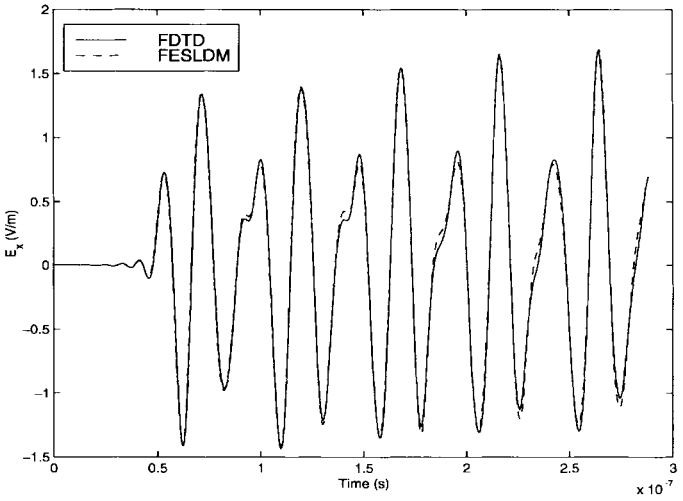

Fig. 7. A comparison of the FESLDM and FDTD response of the air-filled cavity excited by a tapered sine function with a low-pass filter.

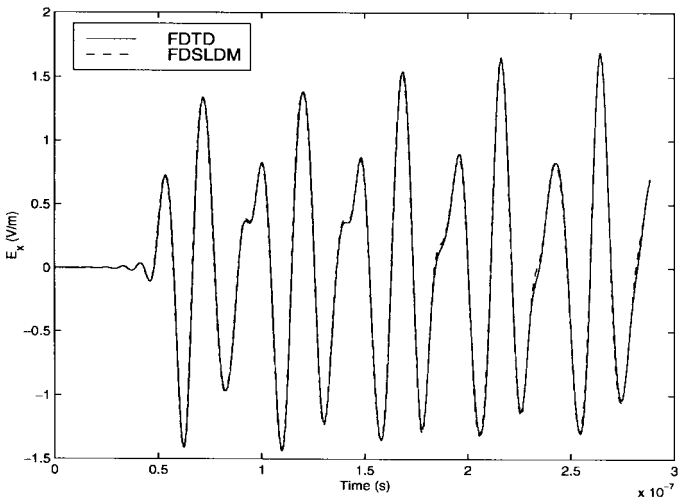

Fig. 8. A comparison of the FDSLDM and FDTD response of the air-filled cavity illuminated by a tapered sine function with a low-pass filter.

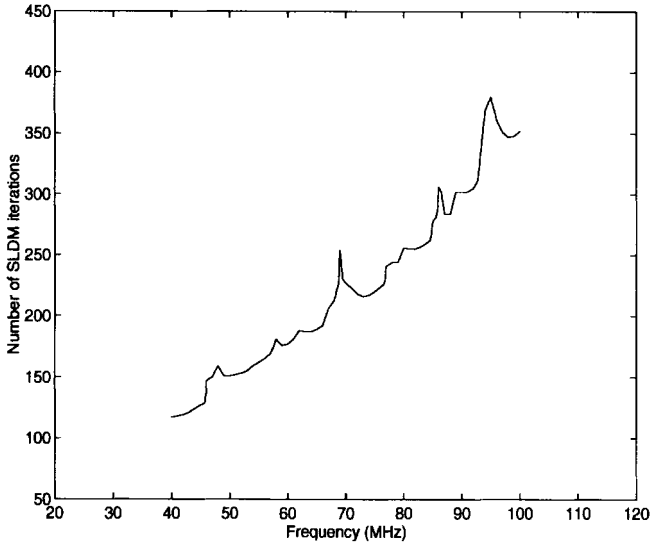

(a)

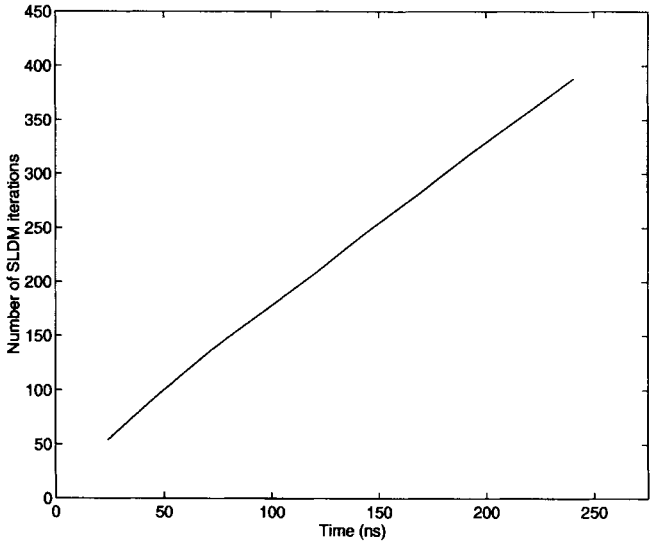

(b)

Fig. 9. Number of SLDM iterations versus: (a) frequency and (b) time.

erations is plotted in Fig. 9. It is seen that as the frequency and time increase, the number of iterations increases accordingly, thus validating the multiple time and frequency procedures.

B. Partially Loaded Dielectric Cavity

A rectangular cavity loaded with a dielectric material is also considered. For the sake of comparison, the same cavity as analyzed in [36] is studied. The problem configuration is illustrated in Fig. 10. The perfect magnetic conductor (PMC) walls are used to reduce the size of the problem domain. The total number of unknowns is 5440. The same source as in the previous section is used to excite the cavity modes. The magnitude of the electric field is computed in a frequency range of 200–500 MHz with a frequency increment of 0.5 MHz while performing the SLDM iterations only at 500 MHz. The total CPU time is 27 s and the result is given in Fig. 11. A comparison of the resonant frequencies with the corresponding results reported in [36] is given in Table III. An excellent agreement is observed.

A multiple time-domain analysis of the cavity is performed next. The time step here is chosen to be 0.030 25 ns with the largest time $t = 30.25$ ns. Again, (29) is used to calculate the field intensity at the center of the cavity. The total CPU time for this case is 235 s. The resonant frequencies obtained from the fast Fourier transform (FFT) of the time domain results are listed in Table IV, and are compared with the corresponding results reported in [36]. A very good agreement is achieved.

The efficiency of the method is further demonstrated by analyzing the cavity, illustrated in Fig. 10, without using the symmetric property of the geometry. The cavity is subdivided into 16, 40, and 12 segments in the x-, y-, and z-directions, respectively, resulting in 20 484 unknowns. A frequency-domain analysis is performed using the SLDM and the results are plotted in Fig. 12. Four resonant frequencies are identical to

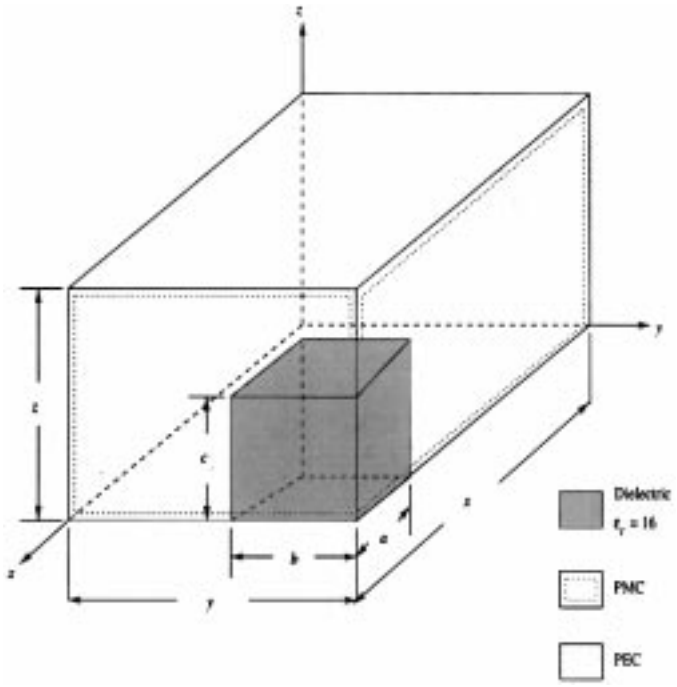

Fig. 10. The problem geometry for the electric field computation of a dielectric loaded microwave cavity with $x = 0.5$ m, $y = 0.2$ m, $z = 0.3$ m, $a = 0.125$ m, $b = 0.075$ m, and $c = 0.175$ m.

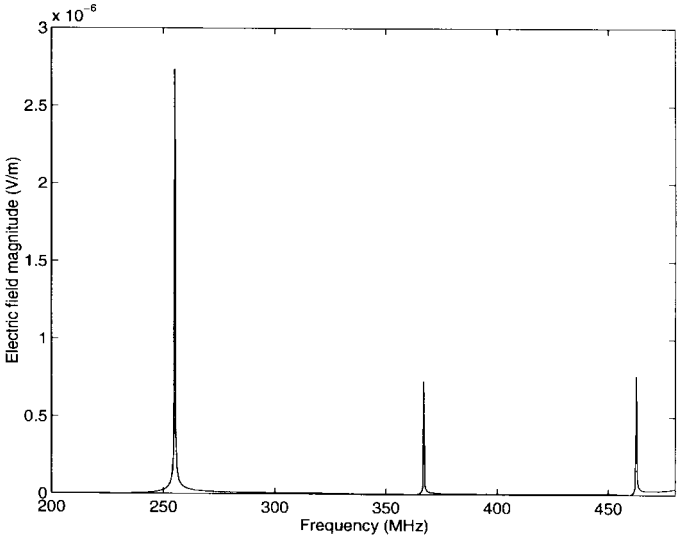

Fig. 11. Typical frequency spectrum of the dielectric-loaded resonant cavity.

TABLE III
RESONANT FREQUENCIES OF A PARTIALLY LOADED CAVITY USING FREQUENCY-DOMAIN ANALYSIS

Mode	1	2	3
FEFD (MHz)	255.1	367.1	462.5
FEM (MHz) [36]	257.9	373.4	475.8
% Difference	1.1	1.7	2.8

the corresponding frequencies obtained when using symmetry. Additionally, the antisymmetric resonant frequencies are also clearly observed in Fig. 12. The total CPU time for this computation is 373 s, of which about 313 s are spent on the first frequency point and only 60 s are spent on the remaining 599 frequency points.

TABLE IV
RESONANT FREQUENCIES OF A PARTIALLY LOADED CAVITY USING TIME-DOMAIN ANALYSIS

Mode	1	2	3
FETD (MHz)	258.2	355.1	452.0
FEM (MHz) [36]	257.9	373.4	475.8
% Difference	0.11	4.9	5.0

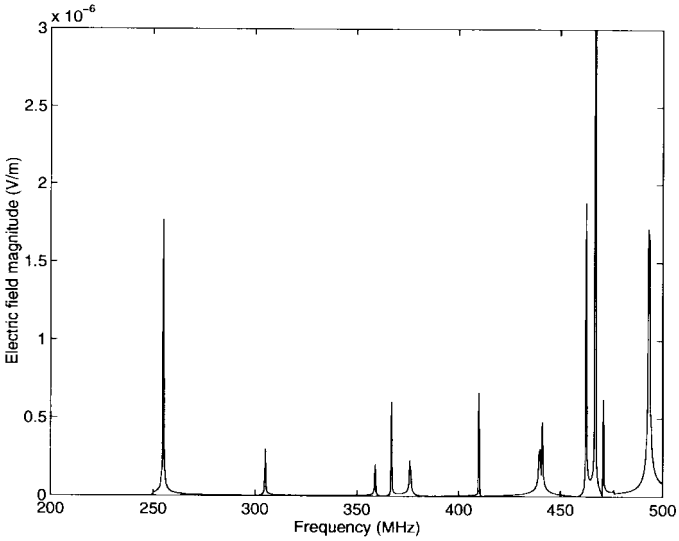

Fig. 12. Typical frequency spectrum of the dielectric-loaded resonant cavity without using symmetry. The resonant frequencies identified from this figure are 255.1, 359.0, 367.1, 376.0, 410.0, 439.5, 441.0, 462.5, 467.0, 471.0, and 493.0 MHz. Those at 255.1, 367.1, 462.5, and 493.0 MHz have been observed in Fig. 13.

V. CONCLUSION

A new efficient time-domain and frequency-domain finite-element solution is proposed. In this technique, the SLDM is applied to the solution of the three-dimensional Maxwell's equations in both frequency and time domains, discretized using the FEM with edge-based elements. The formulation presented in this paper is validated by studying various microwave cavities. Very accurate results are obtained in minimal computational time, illustrating the effectiveness and efficiency of this technique. It is shown that the SLDM is not only computationally fast, but also capable of obtaining solutions at many frequencies and time steps by performing the SLDM iterations only for the largest frequency or time of interest. The problems associated with the mass-lumping procedure for the wave equation is addressed here. It is demonstrated that some inaccuracy is introduced by the mass-lumping technique, although it is not of much significance. Finally, we note that the method can also be extended to deal with lossy problems [38].

REFERENCES

[1] K. S. Yee, "Numerical solution of initial boundary value problems involving Maxwell's equations in isotropic media," *IEEE Trans. Antennas Propagat.*, vol. AP-14, pp. 302–307, May 1966.

[2] A. C. Cangellaris and D. B. Wright, "Analysis of the numerical error caused by the stair-stepped approximation of a conducting boundary in FDTD simulations of electromagnetic phenomena," *IEEE Trans. Antennas Propagat.*, vol. 39, pp. 1518–1525, 1993.
[3] D. Sheen, "Numerical modeling of microstrip circuits and antennas," Ph.D. dissertation, MIT, Cambridge, June 1991.
[4] T. A. Manteuffel and J. A. White, "The numerical solution of the second-order boundary value problem on nonuniform meshes," *Math. Comput.*, vol. 47, pp. 511–535, 1986.
[5] H. Kreiss, T. Manteuffel, B. Shwartz, B. Wendroff, and J. A. White, "Supraconvergent schemes on irregular meshes," *Math. Comput.*, vol. 47, pp. 537–554, 1986.
[6] T. G. Jurgens, A. Taflov, K. Umashankar, and T. G. Moore, "Finite-difference time-domain modeling of curved surfaces," *IEEE Trans. Antennas Propagat.*, vol. 40, pp. 357–366, Apr. 1992.
[7] C. J. Railton, "An algorithm for the treatment of curved metallic laminas in the finite-difference time-domain method," *IEEE Trans. Microwave Theory Tech.*, vol. 41, pp. 1429–1438, Aug. 1993.
[8] R. Holland, "Finite-difference solution of Maxwell's equations in generalized nonorthogonal coordinates," *IEEE Trans. Nucl. Sci.*, vol. NS-30, pp. 4589–4591, Dec. 1983.
[9] K. K. Mei, A. Cangellaris, and D. J. Angelakos, "Conformal time-domain finite-difference method," *Radio Sci.*, vol. 19, pp. 1145–1147, 1984.
[10] J. F. Lee, R. Palendech, and R. Mittra, "Modeling three-dimensional discontinuities in waveguides using nonorthogonal FDTD algorithm," *IEEE Trans. Microwave Theory Tech.*, vol. 40, pp. 346–352, Feb. 1992.
[11] T. Kashiva, T. Onishi, and I. Fukai, "Analysis of microstrip antennas on a curved surface using the conformal grids FDTD method," *IEEE Trans. Antennas Propagat.*, vol. 42, pp. 423–426, Mar. 1994.
[12] M. Fusco, M. Smith, and L. Gordon, "A three-dimensional FDTD algorithm in curvilinear coordinates," *IEEE Trans. Antennas Propagat.*, vol. 39, pp. 1463–1471, Oct. 1991.
[13] S. Gedney, F. Lansing, and D. Rascoe, "Full-wave analysis of microwave monolithic circuit devices using a generalized Yee algorithm based on an unstructured grid," *IEEE Trans. Microwave Theory Tech.*, vol. 44, pp. 1393–1400, Aug. 1996.
[14] S. Gedney and F. Lansing, "A parallel planar generalized Yee algorithm for the analysis of microwave circuit devices," *Int. J. Numer. Modeling*, vol. 8, pp. 249–264, May 1995.
[15] A. C. Cangellaris, C. C. Lin, and K. K. Mei, "Point-matched time domain finite-element methods," presented at the Nat. Radio Sci. Meeting, Boston, MA, June 1984.
[16] ———, "Point-matched time domain finite-element methods for electromagnetic radiation and scattering," *IEEE Trans. Antennas Propagat.*, vol. AP-35, pp. 1160–1173, Oct. 1987.
[17] C. C. Lin and K. K. Mei, "Time domain absorbing boundary condition in lossy media," presented at the Int. IEEE/Antennas Propagat. Soc. Symp., Boston, MA, June 1984.
[18] J. F. Lee, R. Lee, and A. C. Cangellaris, "Time-domain finite-element methods," *IEEE Trans. Antennas Propagat.*, vol. 45, pp. 430–442, Mar. 1997.
[19] S. L. Ray, N. K. Madsen, and J. C. Nash, "Finite-element analysis of electromagnetic aperture coupling problems," presented at the North American Radio Sci. Meeting, June 1985.
[20] J. B. Grant and N. K. Madsen, "GEM3D-A time domain three-dimensional, linear finite-element modeling," presented at the Nat. Radio Sci. Meeting, Boulder, CO, Jan. 1986.
[21] D. R. Lynch and K. D. Paulsen, "Time-domain integration of Maxwell equations on finite-element," *IEEE Trans. Antennas Propagat.*, vol. 38, pp. 1933–1942, Dec. 1990.
[22] A. Bossavit and I. Mayergoys, "Edge elements for scattering problems," *IEEE Trans. Magn.*, vol. 25, pp. 2816–2821, July 1989.
[23] G. Mur, "The finite-element modeling of three-dimensional time-domain electromagnetic fields in strongly inhomogeneous media," *IEEE Trans. Magn.*, vol. 28, pp. 1130–1133, Mar. 1992.
[24] K. Mahadevan, R. Mittra, D. Rowse, and J. Murphy, "Edge-based finite-element frequency and time domain algorithms for RCS computation," in *Proc. IEEE Antennas Propagat. Symp. Dig.*, vol. 3, Ann Arbor, MI, June 1993, pp. 1680–1683.
[25] J. T. Elson, H. Sangani, and C. H. Chan, "An explicit time-domain method using three-dimensional Whitney elements," *IEEE Microwave Guided Wave Lett.*, vol. 7, pp. 607–610, Sept. 1994.
[26] J. F. Lee, "WETD: A finite-element time-domain approach for solving Maxwell's equations," *IEEE Microwave Guided Wave Lett.*, vol. 4, pp. 11–13, Jan. 1994.
[27] Z. S. Sacks and J. F. Lee, "A finite-element time-domain method using prism elements for microwave cavities," *IEEE Trans. Magn.*, vol. 37, pp. 519–527, Nov. 1995.
[28] M. F. Wong, O. Picon, and V. F. Hanna, "A finite-element method based on Whitney forms to solve Maxwell equations in the time-domain," *IEEE Trans. Magn.*, vol. 31, pp. 1618–1621, May 1995.
[29] M. Feliziani and F. Marradei, "Hybrid finite-element solutions of time dependent Maxwell's curl equations," *IEEE Trans. Magn.*, vol. 31, pp. 1330–1335, May 1995.
[30] S. D. Gedney and U. Navsariwala, "An unconditionally stable finite-element time-domain solution of the vector wave equation," *IEEE Microwave Guided Wave Lett.*, vol. 5, pp. 332–334, Oct. 1995.
[31] M. Zunoubi, J. M. Jin, and W. C. Chew, "A spectral Lanczos decomposition method for solving axisymmetric low-frequency electromagnetic diffusion by the finite-element method," *J. Electromagnetic Waves Applicat.*, vol. 11, pp. 1389–1406, 1997.
[32] ———, "The spectral Lanczos decomposition method for solving three-dimensional low-frequency electromagnetic diffusion by the finite-element method," in *Proc. IEEE APS-URSI Symp.*, Montreal, P.Q., Canada, July 1997, p. 39.
[33] V. Druskin and L. Knizhnerman, "Spectral approach to solving three-dimensional Maxwell's diffusion equations in the time and frequency domains," *Radio Sci.*, vol. 29, no. 4, pp. 937–953, Aug. 1994.
[34] J. Jin, *The Finite Element Method in Electromagnetics.* New York: Wiley, 1993.
[35] B. N. Parlett, *The Symmetric Eigenvalue Problems.* Englewood Cliffs, NJ: Prentice-Hall, 1980.
[36] I. Bardi, O. Biro, K. Preis, G. Vrisk, and K. R. Richter, "Nodal and edge element analysis of inhomogeneously loaded 3-D cavities," *IEEE Trans. Magn.*, vol. 28, pp. 1142–1145, 1992.
[37] L. B. Jackson, *Digital Filters and Signal Processing.* Norwell, MA: Kluwer, 1989.
[38] M. Zunoubi, J. M. Jin, and W. C. Chew, "Spectral Lanczos decomposition method for time-domain and frequency-domain finite-element solution of Maxwell's equations," *Electron. Lett.*, vol. 34, no. 4, pp. 346–347, 1998.

Mohammad R. Zunoubi (S'91–M'96) received the B.S. with honors and M.S. degrees in electrical engineering from the University of Mississippi, University, in 1989 and 1991, respectively, and the Ph.D. degree in electrical engineering from Mississippi State University, Mississippi State, in 1996.

From 1989 to 1992, he was a Research Assistant in the Department of Electrical Engineering, University of Mississippi. From 1992 to 1996, he was a Research Assistant and Teaching Assistant in the Department of Electrical and Computer Engineering, Mississippi State University. Since September 1996, he has been a Post-Doctoral Research Fellow at the Center for Computational Electromagnetics, University of Illinois at Urbana-Champaign. His research interests include the areas of computational electromagnetics, antennas, microwaves, and electromagnetic compatibility.

Kalyan C. Donepudi received the B.Tech. degree in electrical engineering from the Nagarjuna University, Nagarjuna, India, in 1995, the M.S. degree from the University of Illinois at Urbana-Champaign, in 1998, and is currently working toward the Ph.D. degree in electrical engineering.

His research interests are in general areas of computational electromagnetics.

Jian-Ming Jin (S'87–M'89–SM'94) received the B.S. and M.S. degrees in applied physics from Nanjing University, Nanjing, China, in 1982 and 1984, respectively, and the Ph.D. degree in electrical engineering from the University of Michigan at Ann Arbor, in 1989.

He joined the faculty of the Department of Electrical and Computer Engineering, University of Illinois at Urbana-Champaign (UIUC), in 1993, after working as a Senior Scientist at Otsuka Electronics, Inc., Fort Collins, CO. He is currently an Associate Professor of electrical and computer engineering and Associate Director of the Center for Computational Electromagnetics, UIUC. He has published over 70 articles in refereed journals and several book chapters, authored *The Finite Element Method in Electromagnetics* (New York: Wiley, 1993) and *Electromagneitc Analysis and Design in Magnetic Resonance Imaging* (Boca Rataon, FL: CRC Press, 1998), and co-authored *Computation of Special Functions* (New York: Wiley, 1996). His current research interests include computational electromagnetics, scattering and antenna analysis, electromagnetic compatibility, and magnetic resonance imaging. He is a member of the Editorial Board of *Electromagnetics Journal*.

Dr. Jin is a member of Tau Beta Pi and Commission B of USNC/URSI. He serves as an associate editor of the IEEE TRANSACTIONS ON ANTENNAS AND PROPAGATION. He was a recipient of the 1994 National Science Foundation Young Investigator Award, 1995 Office of Naval Research Young Investigator Award, and 1997 Junior Xerox Research Award presented by the UIUC College of Engineering.

Weng Cho Chew (S'79–M'80–SM'86–F'93) was born on June 9, 1953, in Malaysia. He received the B.S. degree, both the M.S. and Engineer's degrees, and the Ph.D. degree from the Massachusetts Institute of Technology, Cambridge, in 1976, 1978, and 1980, respectively, all in electrical engineering.

From 1981 to 1985, he was with Schlumberger-Doll Research, Ridgefield, CT, where he was a Program Leader and a Department Manager. From 1985 to 1990, he was an Associate Professor at the University of Illinois at Urbana-Champaign, and is currently a Professor teaching graduate courses in waves and fields, inhomogeneous media, and theory of microwave and optical waveguides, and supervising a graduate research program. From 1989 to 1993, he was the Associate Director of the Advanced Construction Technology Center, University of Illinois at Urbana-Champaign, where he is currently the Director of the Center for Computational Electromagnetics and the Electromagnetics Laboratory. His name is listed in the university's *List of Excellent Instructors*. He has authored *Waves and Fields in Inhomogeneous Media* (New York: Van Nostrand, 1990), published over 175 scientific journal articles, and presented over 200 conference papers. His recent research interest has been in the area of wave propagation, scattering, inverse scattering, and fast algorithms related to scattering, inhomogeneous media for geophysical subsurface sensing, and nondestructive testing applications, He has also previously analyzed electrochemical effects and dielectric properties of composite materials, microwave and optical waveguides, and microstrip antennas. He is an associate editor of *Journal of Electromagnetic Waves and Applications* and *Microwave Optical Technology Letters.* He was also an associate editor with the *International Journal of Imaging Systems and Technology*, and has been a guest editor of *Radio Science*, *International Journal of Imaging Systems and Technology*, and *Electromagnetics.*

Dr. Chew is a member of Eta Kappa Nu, Tau Beta Pi, URSI Commissions B and F, and the Society of Exploration Geophysics. He has been an Ad Com member of the IEEE Geoscience and Remote Sensing Society, and is currently an associate editor of the IEEE TRANSACTIONS ON GEOSCIENCE AND REMOTE SENSING. He was a National Science Foundation (NSF) Presidential Young Investigator in 1986.